Role of Magnus effect in cell separation using dielectrophoresis

Saeed Izadi, Shibabrat Naik, Rafael V. Davalos

May 10, 2013

Abstract

The dielectrophoretic cell separation and the underlying electro-hydrodynamics is studied in the light of a single biological particle in a simplified geometry of electrodes. We propose and test a hypothesis related to the electro-rotation and preferential motion of cells observed in experiments. This work investigates the scaling of the forces and displacements to test the hypothesis and attempts a theoretical explanation of rotational motion. The phenomena of electro-rotation observed in experiments and bio-medical devices have been only used to answer how the rotation occurs. We present a scaling analysis of the electro-rotation and explore its influence on the trajectory in a simplified domain.

1 Introduction

Controlling and understanding the dynamics of small particulates in the size range from approximately one micron (10^{-6} m) up to one millimeter (10^{-3} m) have gained interest due to applications in packed and fluidized bed reactors, powder coating machines, electrostatic precipitators, electronic chip design and more recently characterization, handling and manipulations of cells, viruses and DNA molecules for bio-medical science and engineering. It is now well-established to manipulate and control sub-micron particle using electrokinetics and dielectrophoresis [1], [2]. On one side, these methods are applied to calculate dielectric properties of cells or biological species of interest and form a library of cell's electrical parameters and thus on theoretical interest. While on the other hand, the knowledge of the dielectric properties are extensively required to manipulate and isolate cells for bio-medical devices which is of interest from an application aspect.

Dielectrophoresis(DEP), the motion of a particle due to its polarization in the presence of a non-uniform electric field, has been used to manipulate biological cells including fluid mixing, separation, enrichment, detection and to calculate specific electrical properties. The DEP force is dependent on, as we will discuss later, the volume of the particle, the polarizability of the suspending medium, the dielectric properties of the particle and the gradient of the electric field. Further more, the direction of the DEP force is a governing mechanism in the applications where by a positive DEP implies particles are attracted to electric field intensity maxima and repelled from minima and vice-versa for negative DEP. This is schematically shown in Fig. 1

as particles show distinct motion depending on the whether DEP is positive or negative. The dielectrophoretic force can either be positive or negative depending on the applied frequency of the electric field and the electrical properties of the cell. Hence the particles which are more polarizable than the surrounding medium is attracted towards the stronger field and the particles with low polarizability are directed away from the stronger field region.

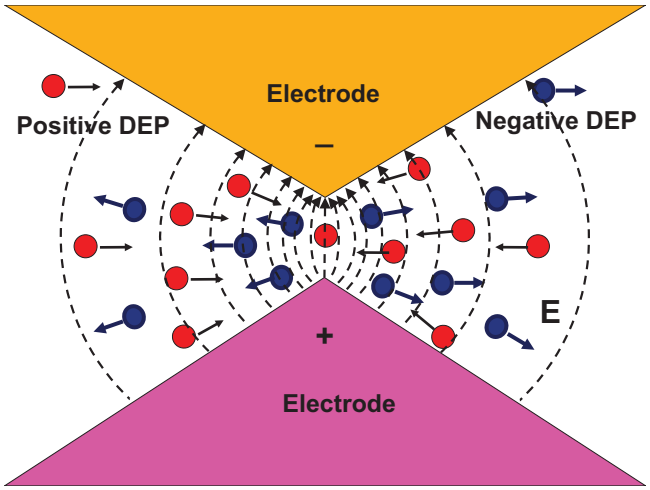

Figure 1: Schematic showing the concept of using dielectrophoresis for isolating cells with different dielectric properties[3]

Although the primary mechanism is based on the dielectric properties of the cells, the system under analysis involves other physics like hydro-dynamics, Brownian motion, rigid body rotation, joule heating. From the perspective of applications, the magnitude and direction of these forces are numerically simulated, experimentally tested or analytically solved for a specific geometry. The literature [4] and [5] from this point of view deal with characterizing all the forces and torques for patterning, manipulation and isolation of biological cells in aqueous medium. In the full scale model, this is considered as the dynamics of a elastic body with a some dielectric signature which is experiencing electro-hydrodynamical forces. In other side of the literature, there are application oriented approaches [6], [7], [8], [9], [3] which deal with electrode configuration, characterizing and distinguishing specific cell types based on dielectrophoresis. In the experiments performed in [10], three important features of a cell's motion in dielectrophoretic system was noticed. Repulsion of the cells from the electrodes, stirring of the dielectric fluid and the rotation of the cells about an axis through their centers.

Amongst all the forces that are encountered in a typical dielectrophoretic system, the most puzzling phenomena is that of cell rotation [10]. In this context the cells spin about an axis normal to the electric field lines. The work in [10] provides evidence that the rate of rotation is

dependent on the applied frequency of the field and the conductivity of the particle. The work in [10] presents it to be useful for differentiating cells based on age as they have different rotative responses. One of the possible causes provided in the literature is that of charge transfer process but a scale smaller that at which rotation is observed. In a recent study [11], self-rotation of cells in an irrotational AC electric field is reported and is hypothesized to be due to the uneven distribution of mass in cells.

Although numerous studies are undertaken to clarify the cause of cell rotation and its dependence on dielectric properties of the system, yet no rigorous analytical explanation has been proposed to characterize the dynamics of cells due to rotational motion. Rotation can substantially affect the flow streamlines pattern around the suspending objects in fluid. Any change in pressure distribution as a result of change in streamlines will affect the trajectory of cells. This phenomenon, known as Magnus effect, is extensively studied at macro-scale to explain commonly observed deviations from the typical trajectories or paths of spherical objects. However, whether rotation can justify preferential motions of cells in electrical fields with symmetric geometries at micro-scale [6] is still unanswered. Accurate prediction of cells trajectories are of fundamental importance in contactless dielectrophoresis where cells are separated and manipulated due to their dynamical response to the electric field.

In the following work, we suggest to isolate the rotational motion and provide an explanation for the observed phenomena. In particular, we investigate how rotation contributes to the particles deviation from their original trajectory at micro-scale. Accordingly, we study the Magnus effect to provide a sound understanding of the preferential motion of cells in complicated channels at a micro-scale.

2 Particle dynamics

(a) Dielectrophoresis

The time-average Dielectrophoresis (DEP) force acting on a spherical particle in a non-uniform electric field is given by

$$\mathbf{F}_{DEP} = 2\pi\varepsilon_m a^3 Re[K_{CM}]\boldsymbol{\nabla}(\mathbf{E}_{RMS}.\mathbf{E}_{RMS}) \tag{2.1}$$

where ε_m is the absolute permittivity of the suspending fluid(DEP buffer), a is the radius of the particle, $Re[K_{CM}]$ is the real part of a complex factor given by Eqn. 2.2 in terms of the

absolute permittivities of the DEP buffer and the particle.

$$K_{CM}(\omega) = \frac{\varepsilon_p^* - \varepsilon_m^*}{\varepsilon_p^* + 2\varepsilon_m^*} \tag{2.2}$$

where, ε^* is the complex permittivity defined as

$$\varepsilon^* = \varepsilon - \frac{j\sigma}{\omega}$$

ε and ω are the real permittivity and conductivity, respectively with $j^2 = -1$.

The sign of the real part of Eqn. 2.2 determines the direction of the DEP force on a particle while the imaginary part determines the electro-rotational torque on the particle. When an induced dipole sits in a uniform electric field, each charge on the dipole is parallel to the field and hence experiences a torque. If the direction of the field vector changes, induced dipole moment vector realigns itself with the field and hence a particle rotation occurs [11]. The time average torque acting on the particle in a oscillating electric field(A.C) is given by the eqn. 2.3

$$\mathbf{\Gamma}_{DEP} = -4\pi\varepsilon_m a^3 Im[K_{CM}(\omega)]\mathbf{E}_{rms}.\mathbf{E}_{rms} \tag{2.3}$$

(b) Multishell model

Biological particles are inhomogeneous and are modeled using a multi-shell model to account for the combined electrical properties of the membrane and the cytoplasm. The Clasius-Mossotti factor for such a particle is calculated using the effective values of the complex relative permittivity or conductivity. The relative permittivity of a cancer cell is expressed by Eqn. 2.4.

$$\varepsilon_p = \varepsilon_{mem} \frac{\left(\frac{r_p+d}{r_p}\right)^3 + 2\left(\frac{\varepsilon_{cyt}-\varepsilon_{mem}^*}{\varepsilon_{cyt}+2\varepsilon_{mem}^*}\right)}{\left(\frac{r_p+d}{r_p}\right)^3 - 2\left(\frac{\varepsilon_{cyt}-\varepsilon_{mem}^*}{\varepsilon_{cyt}+2\varepsilon_{mem}^*}\right)} \tag{2.4}$$

(c) Drag force

At the small length scales found in microfluidics, viscosity dominates and liquid flow in laminar. Also for simplicity, we consider the particles to be spherical. Therefore, Stokes flow assumptions are valid and the hydrodynamic frictional force due to translation, F_{drag}, and hydrodynamic frictional torque due to rotation, T_f, can be computed from the the Stokes' Law

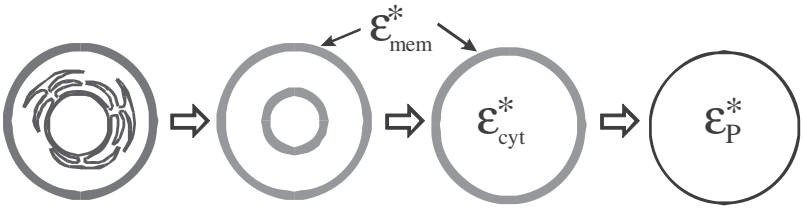

Figure 2: Schematic of converting a nucleated cell to a homogeneous sphere with effective permittivity ε_p^* given by 2.4 which involves representing the endoplasm as a topographical feature followed by a smeared-out cytoplasm surrounded by a membrane of complex permittivities ε_{cyt}^* and ε_{mem}^* respectively [12]

$$F_{drag} = 6\pi\eta a(u_p - u_f) \tag{2.5}$$

$$T_f = 8\pi\eta a^3\Omega \tag{2.6}$$

where η is the viscosity of the medium, a is the particle radius, u_p is the particle velocity, u_f is the medium velocity, T_f is the induced torque and Ω is the electrorotation rate (rad/s).

(d) Buoyancy and gravity

For a particle of density ρ_p suspended in a fluid of density ρ_f, the buoyant force is given by 2.7.

$$\mathbf{F}_b = v(\rho_f - \rho_p)\mathbf{g} \tag{2.7}$$

where $\mathbf{g}$ is the acceleration due to gravity and v is the volume of the particle. To a first order approximation, the velocity due to buoyancy can be estimated as

$$u_p \approx 0.2\frac{d_p^2\rho_p g}{\eta} \tag{2.8}$$

The factor being still smaller in case of biological particles with density close to the dielectrophoretic fluid (or termed as buffer which is an aqueous solution of water and salt). In such systems, the characteristic time scale of acceleration ($\approx 10^{-6}$ s) is much smaller than the time scale of observation in experiments ($\approx 10^{0}$ s). As such, the particles are moving at the terminal velocity and their inertial acceleration can be neglected. In a full-scale numerical model, the acceleration of the particle and of the adjacent fluid and the diffusion of vorticity should be considered [2].

(e) Thermal and Brownian

For a single particle, the deterministic displacement should be greater than that due to the random Brownian motion, to be moving in a deterministic manner during the observation time. The following equation (2.9) approximates the random displacement of a particle with radius a, at temperature T and during the time period t

$$\Delta x = \sqrt{2Dt} = \sqrt{\frac{k_B T}{3\pi a \eta} t} \tag{2.9}$$

where k_B is Boltzman's constant. The Brownian effects becomes meaningless compared to other forces in a dielectrophoretic system especially when the particle size is in the order of microns.

(f) Magnus force

Consider a sphere traveling at a velocity V through an oncoming flow as shown in Fig. 3 (a). If the fluid is viscous, the sphere will experience a drag force. Next, consider a counter-clockwise spinning sphere traveling at a velocity V through an oncoming flow shown in Fig. 3 (b). Once again, the sphere will experience a drag force if the fluid is viscous, however, a pressure difference will emerge as well, resulting in a force normal to the velocity of the sphere. This force is the cause for the curved motion the sphere and is known as the Magnus force. The magnitude of the Magnus has the representation given by Eqn. 2.10.

$$\mathbf{F}_M = 4\pi a^3 \rho_f \left[\vec{\omega} \times (\vec{u}_p - \vec{u}_f)\right] \tag{2.10}$$

where $\vec{\omega}$ is the angular velocity, $\vec{u}_p$ is the particle velocity, $\vec{u}_f$ is the fluid velocity, ρ_f is the fluid density, a is the particle radius.

3 Equations of motion

Combining the physics and the assumptions made in Sec. 2, we can write the equations for the motion of a cell suspended in a dielectric medium with an applied frequency as given by

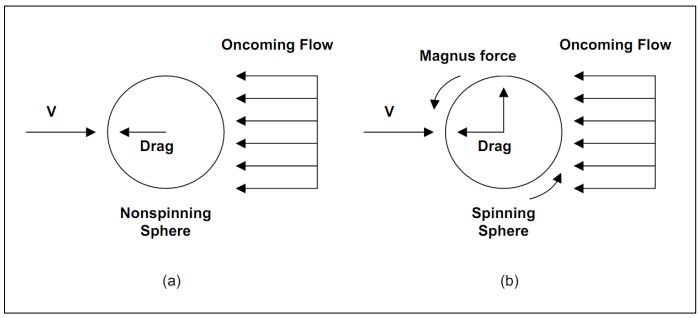

Figure 3: Schematic showing the Magnus effect and the resulting rotation of a spherical particle [13]

Eqn. 3.11.

$$\left.\begin{aligned} m_p \frac{du_r}{dt} &= F_{DEP} + F^r_{drag} \\ m_p \frac{du_t}{dt} &= F_M + F^t_{drag} \\ I_p \frac{d\omega}{dt} &= \Gamma_{DEP} + T_{drag} \end{aligned}\right\} \tag{3.11}$$

Inertial effects being negligible for such a system, the time derivatives of Eqn. 3.11 becomes zero and we can obtain a simple model for the translational and rotational velocities as given by Eqn. 3.12.

$$\left.\begin{aligned} u_r &= \frac{F_{DEP}}{6\pi\eta a} \\ u_t &= \frac{F_M}{6\pi\eta a} \\ \omega &= \frac{\Gamma_{DEP}}{8\pi\eta a^3} \end{aligned}\right\} \tag{3.12}$$

(a) Electrical field calculations

A simplified electrode configuration is one with a cylindrical symmetry which is practically a central wire held coaxially inside an outer cylindrical electrode although there also exists other approximated geometries [14]. In the case of perfect cylindrical symmetry, with the inner electrode of radius r_i at a potential V_1 and concentric to a grounded outer one of radius r_o, the potential V at some intermediate radius, $r_i \leqslant r \leqslant r_o$, from the central axis is:

$$V_{cyl} = V_1 \frac{\ln(r/r_i)}{\ln(r_i/r_o)}$$

For the present study, two coaxial cylinders are considered with positive voltages on the

inner concentric with a grounded outer cylinder (Fig. 4). The analytical solution for the electric field is given by Eqn. 3.13.

$$\mathbf{E}_{cyl} = V_1 \frac{\hat{\mathbf{r}}}{r \ln r_o/r_i} \tag{3.13}$$

4 Results

The numerical values of the variable used in the simulations are defined in Table 1. Numerical studies were performed to build a time-discretized solution of the system of equations. Two coaxial cylinders are considered with positive voltage on the inner concentric with a grounded outer cylinder. The inner cylinder has radius $r_i = 10\mu m$ and the outer has radius $r_o = 1000\mu m$ as shown in Fig. 4. Electrostatic computations were performed for voltages ranging 40-300 V applied on the inner cylinder. The applied frequencies vary from 1-100 KHz. Fluid suspending media (DEP buffer) is characterized in Table 1, and is considered to be at rest. A single spherical two shell cell, (Table 1), is initially placed at the outer cylinder to be translating toward the inner cylinder. The electrostatic force due to the electric field drives the particle in r-direction (invariance along t-axis and z-axis). The particle diameters vary from 15-25 μm, which correspond to typical size of cancer cells.

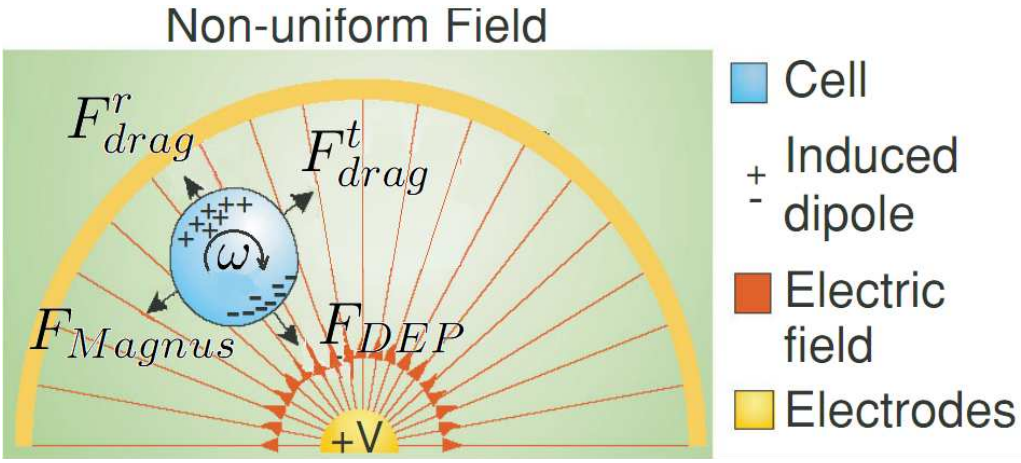

Figure 4: Electrode configuration [15] for which the particles are released from the outer boundary

The analyses are based on the following assumptions. The resulting motion is sufficiently slow so that the Stokesian approximation is valid. To reduce complicated mathematical analysis,

Table 1: Numerical values of the variables

Notation	Name of the paramter	Numerical value used
ρ_p	Density of the particle	1000 kg/m^3
ρ	Density of the DEP buffer	1000 kg/m^3
ε_{mem}	Relative permittivity of the membrane	10-8
ε_{cyt}	Relative permittivity of the cytoplasm	60
ε_b	Relative permittivity of DEP buffer	80
σ_b	Electrical conductivity of DEP buffer	0.01 S/m
μ_b	Dynamic viscosity of DEP buffer	0.001 Pa-s
d_p/a	Diameter/radius of particle (cancer cells)	$d_p = 15 - 20^{-6}$ m
d	Thickness of the cytoplasm	5e-9 m

the mass density of the cell is assumed to be approximately equal to that of the suspending medium (Table. 1). As a result, the gravitational force can be neglected. The time characteristic of acceleration is smaller than 10^{-6} s for cells, which is counted as very small time scale compared to the observation time. The order of time scale in our simulations is 10^{-4} s. In such case, the particles can be considered to move at their terminal velocity where the translational force is balanced by the frictional drag force. Hence, the inertia can be neglected. Furthermore, the effects of Brownian motion becomes insignificant for the size of the particles at the order of μm. Therefore, we overlook the Brownian effects in this work.

The equations of motion are independently solved along radial (r-axis) and tangential (t-axis) directions. From the knowledge of the force on the sphere, it is then possible to determine the velocity at each time step. Integration of the equations of motion then yields a trajectory that describes the position and velocities of the sphere as they vary with time. In r and t directions, the driving forces are DEP and Magnus force and the resisting forces are the Stokes drag force projection along r-axis and t-axis, respectively. As pointed out earlier, the Inertial force is neglected. Therefore, driving and resisting forces are equal at each time step. This yields identical averaged values over time. For the same reason, only the driving forces (DEP and Magnus) are illustrated in the figures for comparisons. Besides, the values for inertial forces produced as a result of the change in velocity are provided in the results, just to re-emphasize that it is inconsiderable.

Figures 5(a)-5(c) show the effect of varying applied voltage and frequency on DEP, Magnus and inertia. As is apparent from the figures, both DEP and Magnus force grow up as the voltage increases from 100V in 5(a) to 300V in 5(c), while the inertia remains negligible for all cases. This is due to the fact that an increased electric field strength drives the particle with higher

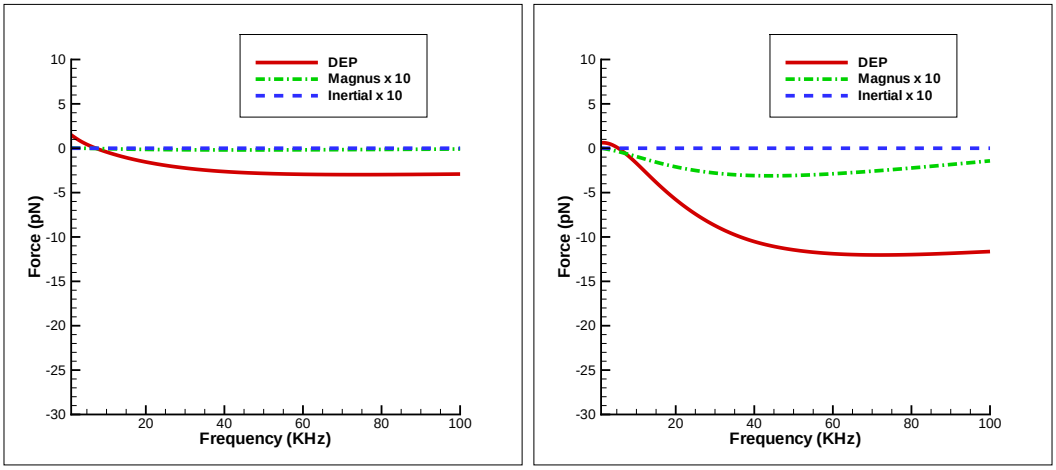

(a) (b)

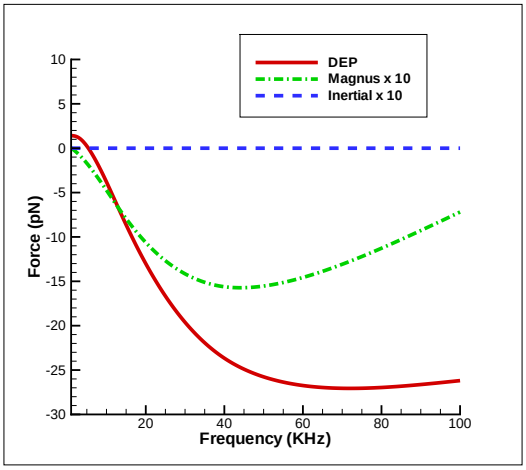

(c)

Figure 5: Scaling plots for different frequencies for varying applied voltage: 5(a) 100V, 5(b) 200V and 5(c) 300V. Diameter is kept fixed at 20 μm.

velocity, which itself magnifies the Magnus force. It is also observed that as frequency increases, DEP force continuously increases whereas the Magnus force increases to some extend and then begins to reduce. This is essentially due to the imaginary part of the eqn. 2.2 that shows a similar up-down trend with change in frequency(6(a)). Likewise, it affects the electro-rotation magnitude, angular velocity and eventually the Magnus force. To provide additional evidence for the behavior of angular velocity in different frequencies, figure 6(b) is provided. As seen, the angular velocity peaks at frequency equal to 10 KHz for different voltages.

The characteristic feature of figures 5(a)-5(c) is the negligibility of Magnus force and inertia compared to DEP. In particular, Magnus force progressively disappears when the voltage is reduced. However, it should be noted that Magnus force acts perpendicular to the DEP force direction. In other words, such relatively smaller force perpendicular to the larger DEP force

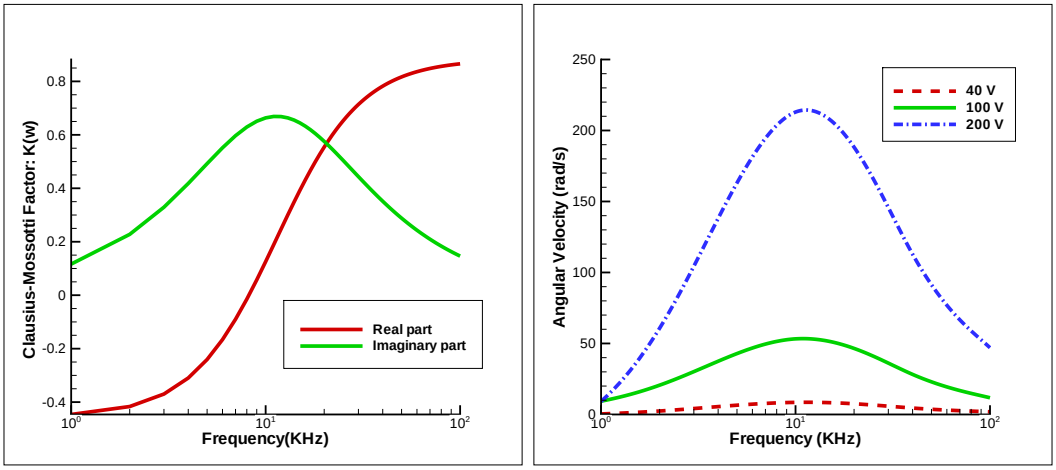

(a) (b)

Figure 6: Left: Real and imaginary parts components of Clausius-Mossotti factor versus frequency. Right: Angular velocity as a function of frequency plotted for various voltages. Diameter is kept fixed at $20\mu m$.

might cause the sphere to curve away from its principal path. This is more closely studied in figures 7(a)-7(c), in which the trajectories of the particle for different voltages and frequencies are illustrated. As expected, the deviation from the original path is negligible for the small voltage of 40 V. However, for voltages as high as 300 V, the displacement in t direction can become larger up to 10% of the total displacement.

The influence of the cell size on the magnus effect is also investigated (figure 4). In general, all of the acting forces in the studied example directly depend on diameter. Specifically, the Magnus force and drag force that dominate in t-direction, vary at different rates by the diameter change. Namely, Magnus force is proportional to a^3, whereas the drag force is proportional to a. This leads to a greater ampilification in Magnus force compared to the drag force by increased diameter, and consequently a greater deviation from the original path.

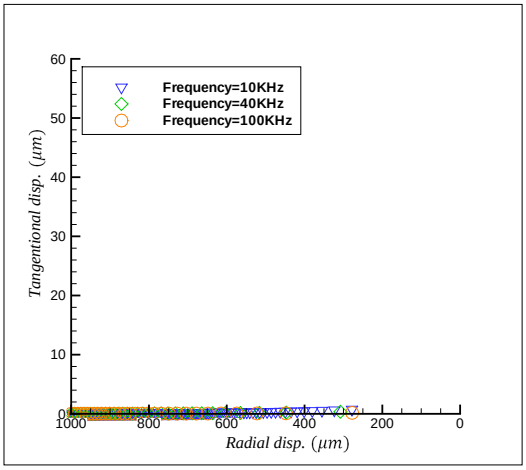

(a)

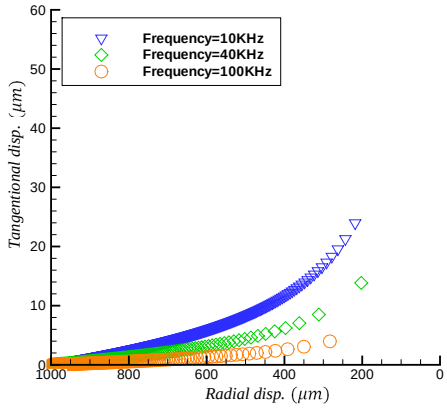

(b)

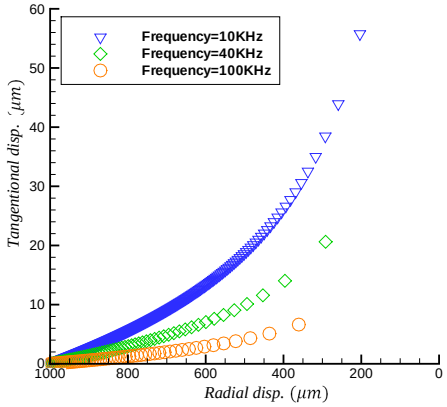

(c)

Figure 7: Trajectory plots for different frequencies for varying applied voltage: 7(a) 40V, 7(b) 200V and 7(c) 300V. The horizontal and vertical axes represent the displacement in along r and t directions, respectively.

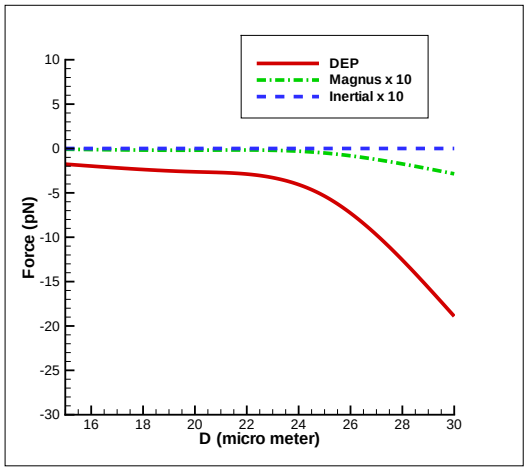

Figure 8: Effect of diameter on acting forces plotted for different voltages.

5 Conclusions and future work

The work presented here discusses the role of Magnus effect to characterize the dynamics of rotating spherical particles in an electrical field. We are able to identify the speeding-up, slowing-down or stopping of the rotation as a function of frequency in the model electrode configuration. This effects are studied for a dielectrophoresis system which is of interest in many practical applications and deals with single and emsemble of biological cells for manipulation and separation. The authors propose this explanation by identifying the crucial factors in the dynamics of a cell's motion using a simplified electrode geometry. This is also an attempt to provide a sound understanding of the preferential motion of cells in complicated channels at a micro-scale. These channels are designed for various applications which have specific requirements for cell isolation and the dielectrophoresis forces are coupled with the geometry due to changing form of electric field.

We hope to present this work as a communication to the electrophoresis community to fill up a gap in theoretical explanation of the cell's rotation. We also plan to extend these ideas in to a project in contactless dielectrophoresis with our supervisor and a post-doc with him.

Acknowledgments

The authors acknowledge sincerely the time and efforts of Alireza Salmanzadeh in providing us with the fundamental ideas and pointing us to important references.

References

[1] Morgan H, Green NG (2003) *AC electrokinetics: colloids and nanoparticles* (Research Studies Press).

[2] Castellanos A, Ramos A, Gonzalez A, Green NG, Morgan H (2003) Electrohydrodynamics and dielectrophoresis in microsystems: scaling laws. *Journal of Physics D: Applied Physics* 36:2584–2597 744CX Times Cited:37 Cited References Count:25.

[3] Yang F, et al. (2010) Dielectrophoretic separation of colorectal cancer cells. *Biomicrofluidics* 4:013204.

[4] Gagnon ZR (2011) Cellular dielectrophoresis: Applications to the characterization, manipulation, separation and patterning of cells. *ELECTROPHORESIS* 32:2466–2487.

[5] Jones T (2003) Basic theory of dielectrophoresis and electrorotation. *IEEE ENGINEERING IN MEDICINE AND BIOLOGY MAGAZINE* 22:33–42.

[6] Shafiee H, Caldwell J, Sano M, Davalos R (2009) Contactless dielectrophoresis: a new technique for cell manipulation. *Biomedical Microdevices* 11:997–1006.

[7] Mulhall HJ, et al. (2011) Cancer, pre-cancer and normal oral cells distinguished by dielectrophoresis. *ANALYTICAL AND BIOANALYTICAL CHEMISTRY* 401:2455–2463.

[8] Chang D, Loire S, Mezic I (2003) Closed-form solutions in the electrical field analysis for dielectrophoretic and travelling wave inter-digitated electrode arrays. *JOURNAL OF PHYSICS D-APPLIED PHYSICS* 36:3073–3078.

[9] Salmanzadeh A, et al. (2013) Investigating dielectric properties of different stages of syngeneic murine ovarian cancer cells. *BIOMICROFLUIDICS* 7.

[10] Pohl HA, Crane JS (1971) Dielectrophoresis of cells. *Biophysical Journal* 11:711 – 727.

[11] Chau LH, et al. (2013) Self-rotation of cells in an irrotational ac e-field in an opto-electrokinetics chip. *PLoS ONE* 8:e51577.

[12] Pethig R (2010) Review article—dielectrophoresis: Status of the theory, technology, and applications. *Biomicrofluidics* 4:022811.

[13] Alek Jezoriek SM (year?) Motions of baseballs and footballs.

[14] H.A.Pohl (1978) *Dielectrophoresis:The behavior of neutral matter in nonuniform electric fields* (Cambridge Monographs on physics).

[15] Joel V (2006) *Dielectrophoresis traps of cell manipulation.*

[16] Ramos A, Morgan H, Green NG, Castellanos A (1998) Ac electrokinetics: a review of forces in microelectrode structures. *Journal of Physics D: Applied Physics* 31:2338.

[17] Jones TB (1995) *Electromechanics of Particles* (Cambridge University Press).